Molecular Architecture of Membranes Involved in Excitation–Contraction Coupling of Cardiac Muscle

Xin-Hui Sun, Feliciano Protasi, Masami Takahashi,* Hiroshi Takeshima,‡ Donald G. Ferguson,§ and Clara Franzini-Armstrong

Department of Cell and Developmental Biology, University of Pennsylvania School of Medicine, Philadelphia, Pennsylvania 19104-6058; *Mitsubishi Kasei Institute of Life Sciences, Tokyo, Japan; ‡Department of Neurochemistry, Tokyo Institute of Psychiatry, Tokyo, Japan; and §Department of Anatomy, Case Western Reserve University, Cleveland, Ohio 44106-4930

Abstract. Peripheral couplings are junctions between the sarcoplasmic reticulum (SR) and the surface membrane (SM). Feet occupy the SR/SM junctional gap and are identified as the SR calcium release channels, or ryanodine receptors (RyRs). In cardiac muscle, the activation of RyRs during excitation–contraction (e–c) coupling is initiated by surface membrane depolarization, followed by the opening of surface membrane calcium channels, the dihydropyridine receptors (DHPRs). We have studied the disposition of DHPRs and RyRs, and the structure of peripheral couplings in chick myocardium, a muscle that has no transverse tubules. Immunolabeling shows colocalization of RyRs and DHPRs in clusters at the fiber's periphery. The positions of DHPR and RyR clusters change coincidentally during development. Freeze–fracture of the surface membrane reveals the presence of domains (junctional domains) occupied by clusters of large particles. Junctional domains in the surface membrane and arrays of feet in the junctional gap have similar sizes and corresponding positions during development, suggesting that both are components of peripheral couplings. As opposed to skeletal muscle, membrane particles in junctional domains of cardiac muscle do not form tetrads. Thus, despite their proximity to the feet, they do not appear to be specifically associated with them. Two observations establish the identity of the structurally identified feet arrays/junctional domain complexes with the immunocytochemically defined RyRs/DHPRs coclusters: the concomitant changes during development and the identification of feet as the cytoplasmic domains of RyRs. We suggest that the large particles in junctional domains of the surface membrane represent DHPRs. These observations have two important functional consequences. First, the apposition of DHPRs and RyRs indicates that most of the inward calcium current flows into the restricted space where feet are located. Secondly, contrary to skeletal muscle, presumptive DHPRs do not show a specific association with the feet, which is consistent with a less direct role of charge movement in cardiac than in skeletal e–c coupling.

CALCIUM is an intracellular messenger in all cell types. In muscle fibers, cytosolic-free calcium concentration regulates contraction and relaxation. The endoplasmic reticulum is a storage compartment for calcium and the sarcoplasmic reticulum (SR)[1] of muscle cells cycles large amounts of calcium at each contraction and relaxation (for a review see Pozzan et al., 1994). Rapid release of calcium from ER and SR occurs through the ryanodine receptor (RyR), a channel with high permeability to calcium, encoded by three different genes with various tissue specificity (for reviews see Sorrentino and Volpe, 1993; Ogawa, 1994). The cytoplasmic domains of RyRs are visible as feet in electron micrographs of skeletal and cardiac muscle fibers (Kawamoto et al., 1986; Inui et al., 1987*a*,*b*; Lai et al, 1988; Block et al., 1988; Anderson et al., 1989; Fleischer and Inui, 1989). The visibility of feet (RyRs) in muscle fibers is due to the fact that they are grouped in ordered arrays at junctional domains of the SR (Bossen et al., 1978; Sommer and Johnson, 1979; Sommer et al, 1991; Franzini-Armstrong, 1994; Franzini-Armstrong and Jorgensen, 1994). RyRs from skeletal and cardiac muscle have the same large tetrameric structure, similar conductance, and pharmacological properties, but they are the products of different genes, and the cardiac receptor is more sensitive to activation by Ca^{2+} (for reviews see Meissner, 1994; Coronado et al., 1994; Ogawa, 1994).

Address all correspondence to C. Franzini-Armstrong, Department of Cell and Developmental Biology, University of Pennsylvania School of Medicine, Philadelphia, PA 19104-6058. Tel.: (215) 898-8046. Fax: (215) 898-9871.

1. *Abbreviations used in this paper*: DHPR, dihydropyridine receptor; e–c, excitation–contraction; RYR, ryanodine receptor; SR, sarcoplasmic reticulum; T, transverse.

Calcium release from the SR of muscle is initiated by depolarization of the surface membrane and its invaginations, the transverse (T) tubules. In skeletal muscle, it is thought that the dihydropyridine receptors (DHPRs) sense the membrane depolarization and, perhaps by direct molecular interaction, induce opening of the RyRs and calcium release from the SR (Schneider and Chandler, 1973; Rios and Brum, 1987; Tanabe et al., 1988; Rios and Gonzales, 1991). Indeed, DHPRs are located in specialized junctional domains of surface membrane/T tubules (Jorgensen et al., 1989; Flucher et al., 1990; Yuan et al., 1991) directly facing the junctional domains of the SR on which feet are located. More importantly, DHPRs are grouped into tetrads, positioned in correspondence of the feet subunits (Franzini-Armstrong and Nunzi, 1983; Block et al., 1988; Franzini-Armstrong et al., 1991; Takekura et al., 1994*a*). This provides a structural basis for a possible functional interaction between RyRs and DHPRs. The junctions which allow this interaction have been named excitation–contraction (e–c) coupling units (Franzini-Armstrong and Jorgensen, 1994), because they are the sites at which the surface membrane electrical signal is transduced into calcium release from the SR.

In cardiac muscle, the situation is more complex. As in skeletal muscle, junctional SR vesicles bearing feet form junctions with the surface membrane (called peripheral couplings) and with T tubules (triads and dyads). In addition, however, feet-bearing domains may exist as extended junctional SR and/or corbular SR. These two terms apply to SR domains which are located internally in the fiber at considerable distance from surface membrane/T tubules, bear arrays of feet/RyRs, and store Ca^{2+} (Jewett et al., 1971; Bossen et al., 1978; Sommer and Johnson, 1979; Dolber and Sommer, 1984; Jorgensen et al., 1988; Sommer et al., 1991; Jorgensen et al., 1993; Junker et al., 1994). Peripheral couplings, dyads, and triads of cardiac and skeletal muscles are structurally and functionally related. The internal calcium release units of cardiac muscle (corbular and/or extended SR) have no counterpart in skeletal muscle.

While the disposition of feet (RyRs) is well described in cardiac muscle, very little is known about the position of DHPRs. There is some evidence for proximity between DHPRs and feet in cardiac muscle (Lewis-Carl et al., 1995) but it is not known whether the two proteins have an opportunity for interacting with each other. We have investigated the structure of peripheral couplings in myocardium of embryonic and young chicks, using antibodies to locate DHPRs and RyRs and thin section and freeze-fracture EM to locate feet and determine if tetrads are present. The results show: (*a*) DHPRs and RyRs are clustered and mostly co-localized in foci at the periphery of the muscle fiber; (*b*) large intramembrane particles are grouped in junctional domains of the surface membrane; and (*c*) distribution of junctional domains is similar to that of foci of DHPRs, and RyRs at various stages of development. We propose that surface domains are located opposite arrays of feet at peripheral couplings and that the large particles are DHPRs. In contrast to skeletal muscle, the junctional particles of cardiac muscle are not arranged in tetrads and their disposition may not be related to that of foot subunits.

Materials and Methods

Antibody Preparation

(*a*) CR2 is a rabbit polyclonal antibody raised against a fragment of rabbit DHPR, derived from a plasmid for the 549 COOH terminus amino acids of DHPR (Yoshida et al., 1992). The antibody was purified by protein A-Sepharose 4B and its reaction with chick cardiac DHPR was determined as below. (*b*) 34C is a mouse monoclonal antibody, generously provided by Drs. J. Sutko and J. A. Airey, which recognizes α, β, and avian cardiac RyR (Airey et al., 1990).

Crude Membrane Fraction

Frozen chick hearts were homogenized in a polytron (set 6, 30 min × 4) in 0.25 M sucrose, 1 mM EDTA, 1 mM phenylmethanesulfonyl fluoride, 1 mM 1,10-phenanthroline, 1 μM pepstatin A, 1 μg/ml antipapain, and 1 μg/ml leupeptin and centrifuged at 9,000 *g* for 20 min. The supernatant was further centrifuged at 186,000 *g* for 30 min and the resulting pellet was suspended in the same solution and stored at −80°C until use.

Purification of DHPRs

The [^{3}H]PN200-110–labeled chick cardiac Ca^{2+} channel were precipitated as in Takahashi and Catterall (1987). Microsomal membranes of chick heart were prelabeled with a saturating concentration of [^{3}H]PN200-110 and solubilized in 1% digitonin in NCH solution (125 mM NaCl, 1 mM $CaCl_2$, and 25 mM Hepes-Tris, pH 7.4) containing a mixture of protease inhibitors (1 mM phenylmethanesulfonyl fluoride, 1 mM 1,10-phenanthroline, 1 μM pepstatin A) at 4°C for 30 min. After removing insoluble material by centrifugation at 175,000 *g* for 45 min, the solubilized material was diluted 1:1 with 20 ml of NCH solution, containing 7 ml of packed wheat germ agglutinin–Sepharose. After a 30-min equilibration at 4°C, the wheat germ agglutinin–Sepharose was packed in a column and washed with 0.1% digitonin in NCH solution, and adsorbed glycoproteins were eluted with 100 mM N-acetylglucosamine in 0.1% digitonin in NCH solution. The [^{3}H]PN200-110–labeled DHPR (2,000 cpm/tube) was incubated with various amounts of CR2 or control rabbit IgG in 0.5% digitonin/NCH solution (final volume 100 μl) for 2 h at 4°C. The antigen–antibody complex was precipitated by adsorption to A-Sepharose (2 mg/tube), washed three times with 0.5% digitonin NCH solution and the radioactivity recovered in the precipitate was determined by liquid scintillation counting. The total amount of the solubilized DHPR was determined by polyethylene glycol precipitation assay.

Immunoblotting

Chick heart membrane proteins (25 μg/lane) were separated by SDS-PAGE linear 4–12% acrylamide gel, transblotted onto nitrocellulose sheet using semi-dry transblotting apparatus (Trans blot SD; Bio-Rad Laboratories, Cambridge, MA); Yoshida et al., 1992). The blot was probed with CR2 antibody (4.5 μg/ml) and then with peroxidase-conjugated goat anti-rabbit IgG (Zymed Laboratories, S. San Francisco, CA). The ECL Western blotting detection reagent (Amersham Corp., Arlington Heights, IL) was used for detection.

Immunohistochemistry

For immunofluorescent labeling, hearts were quickly removed from chicken embryos at 20–21 d of incubation (E20-E21) and from young chicks at 6 and 10 d after hatching (D6-D10). The hearts were cannulated through the aorta and perfused with relaxing solution (80 mM potassium acetate, 10 mM potassium-phosphate buffer, 5 mM EGTA). Portions of left ventricle were frozen in liquid nitrogen-cooled propane. Cryostat sections (12–15-μm thick) were cut at −20°C.

Single Labeling. The sections were incubated for 1-h each in 1% BSA in PBS (BSA/PBS), followed by either CR2 or 34C and by Texas red–conjugated goat anti-rabbit IgG (from Molecular Probes Inc., Eugene, OR) and goat anti-rabbit IgG (from Cappel Laboratories, Cochranville, PA), all diluted in PBS/BSA. In control experiments, cryosections were incubated in 1% BSA/PBS for 2 h, followed by one of the secondary antibodies. For double labeling, the sections were incubated simultaneously with both primary antibodies and then with a mixture of Texas red–conjugated goat

anti-mouse IgG (from Molecular Probes Inc.) and fluorescein-conjugated goat anti-rabbit IgG (from Cappel Laboratories). For control, sections were incubated with either one of the primary antibodies, followed by both secondary antibodies, and both channels were examined to confirm no cross reactivity. The specimens were viewed on a scanning confocal microscope (Bio-Rad MRC-600, Microscience Div., Hemel Hempstead, Hertfordshire, England).

Electron Microscopy

Whole hearts were quickly removed from chicken embryos at E4-E21 and from young chicks at D6-D10. Larger hearts (after E10) were perfused with Ca^{2+}-free solution (0.9% NaCl, 10 mM potassium-phosphate buffer, 10 mM EGTA, pH 7.4), followed by primary fixative (3.5% glutaraldehyde in 0.1 M cacodylate buffer, pH 7.4). Smaller hearts were directly immersed in the Ca^{2+}-free and fixative solutions. Small pieces of glutaraldehyde fixed tissue from left ventricle were post-fixed in 2% OsO_4 in cacodylate buffer for 2 h, block stained in saturated uranyl acetate at 60°C for 4 h, and embedded in Epon 812. Thin sections were stained in 4% uranyl acetate in 50% ethanol and lead.

For freeze-fracture, bundles were similarly fixed in either 3.5 or 6% glutaraldehyde, infiltrated in 30% glycerol, frozen in liquid nitrogen-cooled propane, fractured, shadowed with platinum at 45°, and replicated with carbon in a model 400 Balzers freeze fracture (Balzer, Fürstentum, Liechtenstein). The replicas and thin sections were photographed in a Philips EM 410.

Measurements

Areas of junctions were estimated by measuring the length of arrays of feet in the junctional gap. Assuming that the junction is circular and that images of sections cutting across it (such as those in Figs. 4, *A–D*) represent random chords of such circles, the average measured chord (y) is related to the diameter of the average circle (D) by the equation: $y = \pi D/4$. Since the data showed a trend for increase in size with age of the embryo, and the numbers of samples at different ages were not equal, averages were obtained separately for each age group, and a final average computed from those.

Density of intramembrane particles was estimated for junctional domains and random patches of the surface membrane from counts in chicks at E4 to D10. 73 micrographs with excellent shadow quality (comparable to that shown in Figs. 5, *A–D*) were selected from our collection. In each micrograph, large membrane particles, selected visually, were counted in the specialized domains and in the same number of randomly selected areas of similar size.

The apparent diameter of intramembranous particles was measured at right angle to the platinum shadow. All particles visually identified as "large" in junctional domains were tagged and their diameter measured until a count of 100 was reached. An equal number of random particles (excluding visually identified large ones) was measured in areas immediately adjacent to junctional domains. Approximate height was determined by measuring the length of the platinum-free "shadow" for 50 "large" particles in junctional domains and 50 random particles in their immediate proximity. For a 45° shadowing angle, the height of the particle approximately equals the shadow length.

Results

Embryonic chick myocardium fits the following criteria: (*a*) the availability of specific antibodies for DHPR and RyR; (*b*) simplicity of structure. Chick myocytes have no T tubules and extended junctional SR begins to form a few days after hatching (Sommer et al., 1991). Hence, all junctional SR is located under the plasmalemma in peripheral couplings.

Immunoreactivity of CR2 Antibody with Chick Cardiac DHPR

CR2 immunoprecipitated about 60% of [^{3}H]PN200-110-labeled Ca^{2+} channels solubilized from chick cardiac membranes (Fig. 1). In contrast, control IgG did not precipitate the channel at all.

Polypeptides of 250 and 215 kD were identified as the major antigens in chick cardiac membrane by immunoblotting with CR2 (Fig. 2). These are likely to be the nearly full length α_1 subunit of DHPR and a partial proteolysis product, respectively (Yoshida et al., 1992; De Jongh et al., 1989). The less intense bands at 70 and 62 kD varied from one preparation to another and probably are proteolytic fragments of the α_1 subunit.

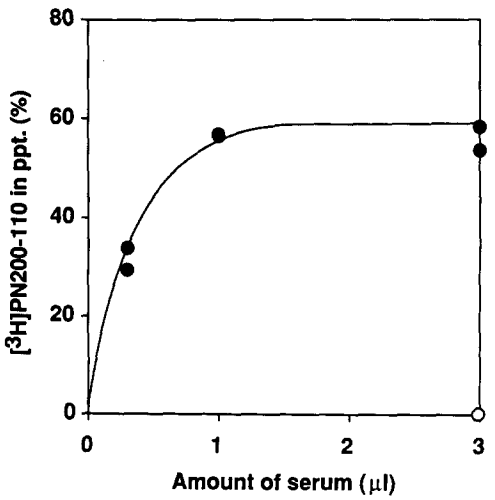

Figure 1. Immunoprecipitation of [^{3}H]PN200-110-labeled chick cardiac Ca^{2+} channels (DHPRs) by CR2 antibody. The labeled channels, solubilized and partially purified, were incubated with the indicated amount of CR2 (●) or control rabbit IgG (○), then precipitated by absorption to protein A–Sepharose. The recovered radioactivity in the precipitate was expressed as percentage of polyethylene glycol-precipitated counts in the supernatant without antibody.

Immunohistochemistry

Immunolabeling at the light microscope level shows that at all ages studied (E20-D10) DHPRs (Fig. 3 *A*) and RyRs (Fig.

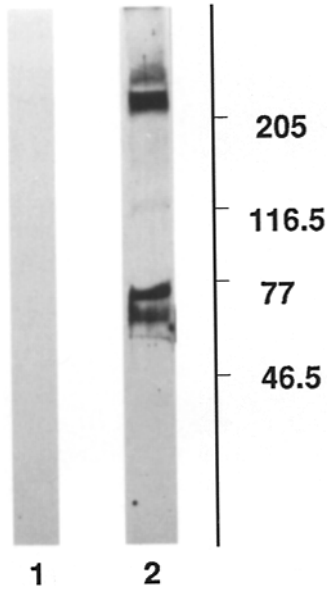

Figure 2. Immunoblotting of α_1 subunit of chick heart with CR2. Membrane proteins (25 μg/lane) were separated by SDS-PAGE, transblotted to nitrocellulose and immunostained with control IgG (lane *1*) or CR2 (lane 2). Molecular mass standards ($M_r \times 10^{-3}$) are indicated on the right.

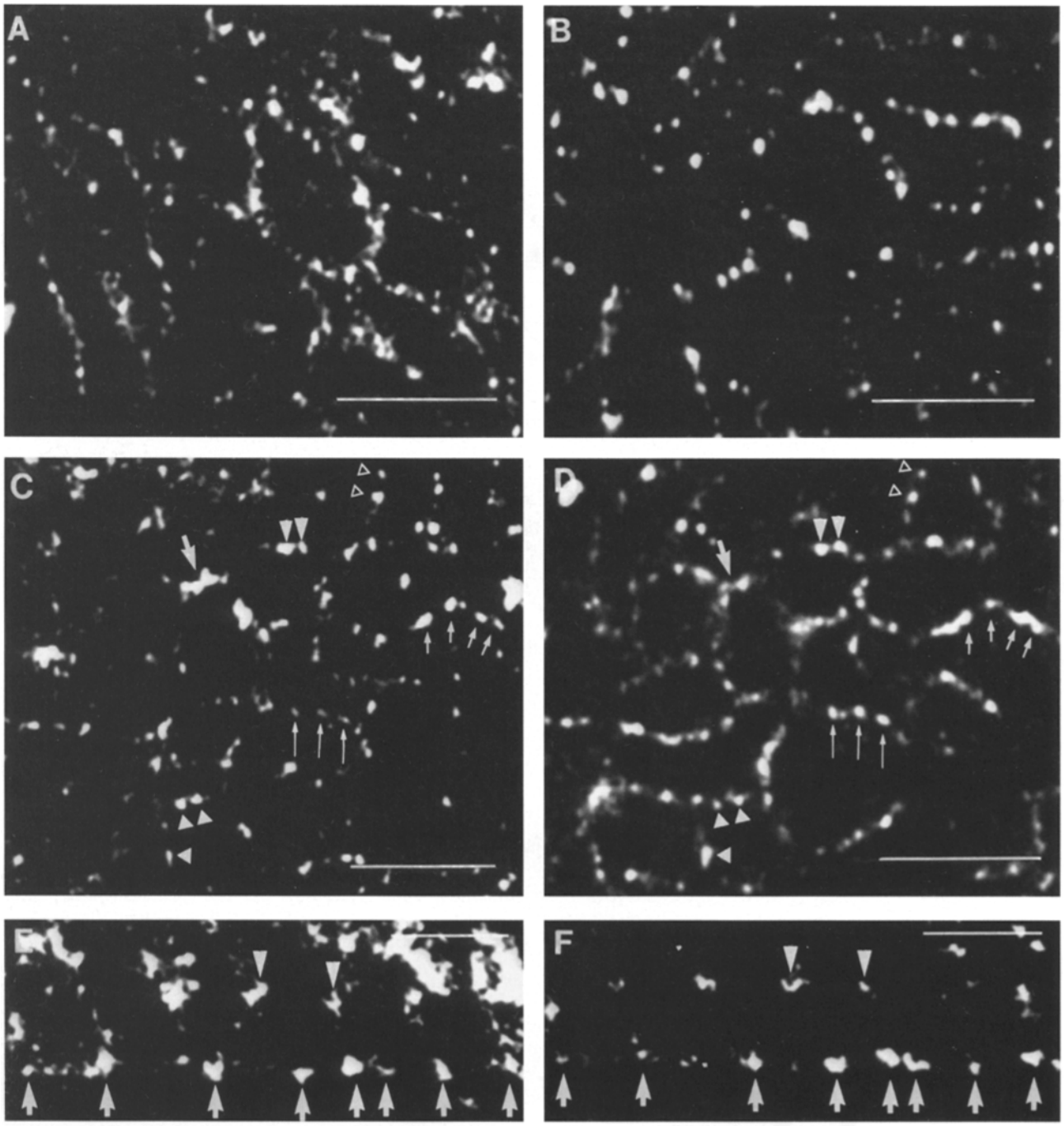

Figure 3. Confocal images of cryosections from the left ventricle of chick myocardium immunolabeled with antibodies against the α_1 subunit of the DHPR (*left*) and RyR (*right*). (*A* and *B*) Cross-sections from a chick at E20. Irregular outlines marked by foci of the two proteins represent the profiles of individual myocytes. (*C* and *D* and *E* and *F*) Double immunolabeling for DHPR and RyR at D10 in cross (*C* and *D*) and longitudinal (*E* and *F*) sections. Several cross-sectional profiles of fibers are seen in *C* and *D*, the edges of a single fiber are shown in *E* and *F*. Corresponding arrows and arrowheads in the double images point to the location of some obviously colocalized foci of RyRs and DHPRs. Many others are found in the images. Bars: (*A–D*) 10 μm; (*E* and *F*) 5 μm.

3 *B*) are located in fairly frequent, discrete clusters (foci) of small size along the cell outlines. The slightly variable and irregular shape of the cells' profiles in cross section corresponds well with that seen in electron micrographs (compare with Fig. 4). In most preparations, the signal from RyR labeling is stronger than from DHPR, and the CR2 antibody tends to give a higher background.

Double immunolabeling for RyRs and DHPRs shows similarity in the staining pattern by the two antibodies, and colocalization of the majority of clusters (see *arrows* and *arrowheads* in Fig. 3, *C* and *D* and *E* and *F*). As noted in the single-labeling experiments, images from the channel for DHPR have more background than those for RyR. Correspondence in the position of DHPRs and RyRs is further

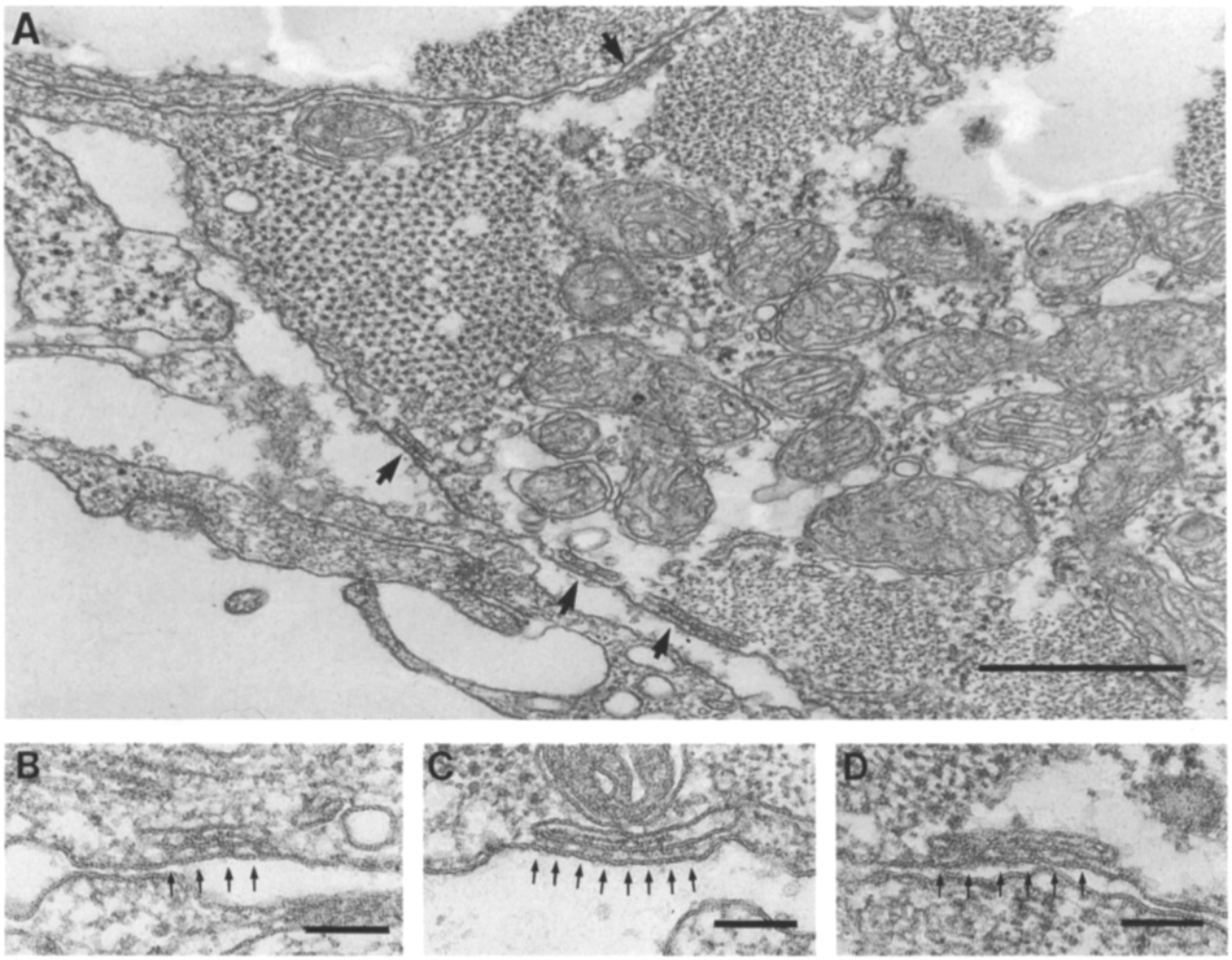

Figure 4. (*A*) Transverse section showing the location of peripheral couplings (*arrows*) at the plasmalemma, from left ventricle at E17. (*B–D*) Details of peripheral couplings, showing content (presumably calsequestrin) of SR vesicles and complete sets of feet, or RyRs (*small arrows*) zippering SR to surface membrane (*B*: E16; *C-D*: E17). Bars: (*A*) 0.5 μm; (*B–D*) 0.1 μm.

confirmed by the observation that both antibodies label foci in colocalized transverse bands in fibers from chicks at D6 and D10 (see below and Fig. 7, *A* and *B*).

Electron Microscopy: Arrays of Feet and Surface Membrane Domains

Peripheral couplings are formed by SR vesicles "zippered" to the surface membrane by arrays of feet (Fig. 4 *A*, *arrows*, and Fig. 4, *B–D*, *small arrows*; see Sommer and Johnson, 1979; Sommer et al., 1991). The lumen of the terminal cisternae is filled with a protein (probably calsequestrin) associated with the junctional SR membrane. In agreement with Sommer et al. (1991), we find that extended junctional SR is not present up to D1, and is still scarce at D6 and D10.

In freeze-fracture replicas, the surface membrane shows domains which have a low content of small and medium sized particles and a high content of large, tall particles (Fig. 5 *A*, *semicircles*; Fig. 5, *B–D*, details). The average density of large particles in these specialized domains is 1,266 ± 252/μm^2 (mean ± 1 SD), n (number of domains) = 114, while the average density of large particles over the rest of the membrane is 109 ± 53/μm^2 (n = 114). The difference is extremely significant (Student's t-test $P < 0.0001$). The "large" particles in the above counts were visually selected. To confirm that this selection does indeed identify a unique set of particles which are taller and larger than average, we measured the size and apparent height of large particles in peripheral couplings, versus those of the random population (see methods). The apparent diameter of visually selected large particles in peripheral couplings is 8.5 ± 0.1 nm, the diameter of random particles is 5.8 ± 0.1 nm (mean ± 1 SEM, number of particles, n = 100). The apparent height (see Materials and Methods) for the large particles is 9.6 ± 0.2 nm (n = 50) while the height of random particles is 5.1 ± 0.2 nm (n = 50). Differences in diameter and height between the "large" and random groups are extremely significant (student's t-test $P < 0.0001$).

Relationship between Surface Membrane Domains and Arrays of Feet

Three observations establish a correlation between arrays of

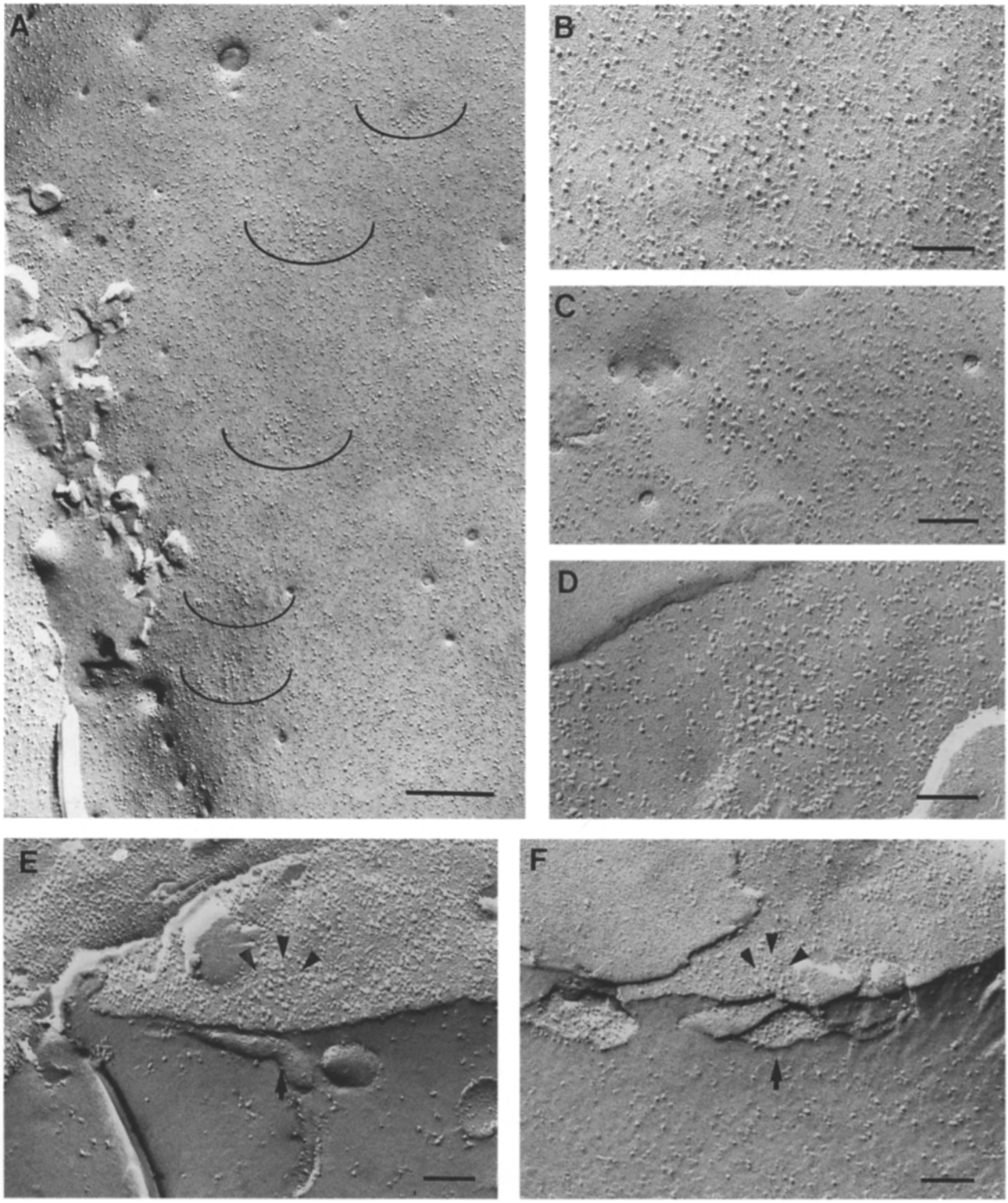

Figure 5. Freeze-fracture through the surface membrane of muscle fibers from left ventricle at E14 (*A*), E4 (*B*), D1 (*C–E*), and D10 (*F*). The longitudinal axis of the muscle fiber in *A* is vertical, and the spacings between junctional domains (*semicircles*) along the longitudinal axis are variable. The large particles in the junctional domains are better visible at higher magnification (*B–D*). Density of large particles is approximately 12-fold higher in the domains than in the rest of the plasmalemma. In *E* and *F* the fracture plane breaks from the surface membrane (upper half of the image) to the fiber interior in the middle of the two peripheral couplings. Two SR vesicles (*arrows*) are located immediately below the two junctional domains (delimited by arrowheads). Bars: (*A*) 0.5 μm; (*B–F*) 0.1 μm.

feet and the surface membrane domains containing large particles. First, all peripheral SR vesicles are components of peripheral couplings and an association between domains and peripheral SR is directly observed. Fig. 5 (*E* and *F*) show two images in which the fracture plane breaks from the surface membrane into the fiber interior at the level of a specialized domain. An SR vesicle (*arrows*) is immediately below the two patches of membrane (*arrowheads*) containing a high density of large particles (1,781/μm^2 for Fig. 5 *E* and 1,353/μm^2 for Fig. 5 *F*).

Secondly, the disposition of peripheral couplings and surface membrane domains show similar maturation-dependent order. A higher proportion of both structures is located at the Z line or within a short distance from it at D6 and D10 than before hatching. These data are further discussed in the next section.

The third observation is indirect: the areas covered by assemblies of feet in the junctional (j) SR membrane and those occupied by large particles in the surface membrane are of approximately equal size. The size of jSR membrane was estimated as described in the methods section, and the areas of surface membrane domains were measured directly from the images. From 457 peripheral couplings, measured in myocardia at E6 to D1, we calculate an average area of 16.6 $\times$ $10^{-3}/\mu m^2$ for the junctional SR. From 268 surface domains, at E6 to D1, we obtain an average area of 17.7 $\times$ $10^{-3}/\mu m^2$. Unfortunately, the two sets of data cannot be compared by a standard non parametric test, because while the freeze fracture data for membrane domains recorded the natural variability in size of the membrane patches, the thin section data for the peripheral couplings recorded both the natural variability and an additional variability due to the position of the measured chord relative to the circle (plane of section effect).

Based on the above findings, the specialized surface membrane domains are called "junctional domains," because they participate in the formation of peripheral couplings.

Correlation between Electron Microscopy and Immunohistochemistry

We have established that clusters of DHPRs and RyRs are colocalized and that junctional domains of the surface membrane correspond to sites of peripheral couplings. Here we strengthen the correlation between these various aspects of the SR-surface junctions by showing that the positions of co-clusters of RyR-DHPR, of feet arrays and of junctional domains change in the same manner during differentiation. Before hatching, there is no obvious periodicity in these positions. Fig. 6 (*A–C*) compare the disposition of junctional domains in a freeze-fracture replica at E21, with that of clusters of DHPRs and RyRs from immunolabeled fibers at E20. In the immunolabeled images (Fig. 6, *A* and *B*), the positions of DHPRs and RyRs foci are random, i.e., the spacings between foci at the fiber edge are variable (between arrows) and in grazing views of the surface (*arrowheads*) there is no apparent order. In freeze-fracture (Fig. 6 *C*) we do not detect an obvious banding pattern in the disposition of junctional domains (*semicircles*). A few days after hatching, on the other hand, the situation is dramatically different (Fig. 7, *A–C*). Double immunolabeling of fibers at D6 shows periodic and colocalized positioning of clusters of DHPRs (Fig. 7 *A*) and RyRs (Fig. 7 *B*) at the fibers' edges (*arrowheads*). Where the surface membrane is parallel to the focal plane of the microscope, foci are seen to form transversely arranged bands at the fiber surface (Fig. 7, *A* and *B*). The distances between the bands labeled by either antibody vary between ~2–3 μm in various preparations and thus represent sarcomeric spacings. This is confirmed by comparing the above measurements with images from thin sections, freeze-fractures, and a section stained with an antibody against α-actinin, where the same range of sarcomere lengths were observed. Cross-sections (see Fig. 3, *C* and *D*) confirm that foci of the two proteins are located at the fiber periphery. In freeze-fracture of fibers at D6, most of the junctional domains (semicircles) are located within narrow transverse strips at the level of the Z lines (Fig. 7 *C*, *arrows*).

In some fibers, particularly at D10, junctions are predominantly located on either side of the Z line. This again is helpful in establishing a correlation between data from immunolabeling, freeze-fracture, and thin section. Fig. 8 (*A* and *B*) show doublets of DHPR and RyR foci along the edges of two different immunolabeled muscle fibers (*double arrows*). Fig. 8 *C* shows paired positioning of junctional domains (*semicircles*) on either side of the Z lines (*arrows*) in a freeze fracture image. In Fig. 8 *D*, from a thin section, five of seven visible peripheral couplings (*arrows*) are located in proximity of the Z lines, but not directly on it.

The above observations are supported by determining the position of arrays of feet (determined from thin sections, *TS*), and of membrane domains (determined in freeze-fracture, *FF*) relative to the sarcomere at E18 versus D6 and 10 (Fig. 9). Distances from the Z line are given as a percentage of sarcomere length measured in the same images (1.7–2.3 μm). This standardizes variations between fibers fixed at slightly different lengths and corrects for differential shrinkages during procedures for thin section and freeze-fracture. The first two bins represent the Z line and the I band, the rest the A band. Both before hatching (E18) and after hatching (D6 and D10), there is a clear tendency for a high frequency of junctions at the Z lines and opposite the I bands. However, at earlier ages, junctions tend to be scattered as much over the A band as in proximity of the Z lines. This data supports the qualitative observations from the images of Figs. 6–8.

Comparison of Junctional Domains from Cardiac and Skeletal Muscle

e–c units in skeletal and cardiac muscle have two major features in common, but also have one very important difference. In both muscles, e–c units have co-localized clusters of DHPRs and RyRs and a correspondence between ordered arrays of feet and junctional membrane domains containing large particles. However, while the junctional particles in skeletal muscle are arranged in groups of four (tetrads) and form extended arrays with spacings directly related to those of feet (Block et al., 1988; Takekura et al., 1994*a*), the junctional particles of cardiac muscle have a random arrangement within the specialized junctional domains. Fig. 10 (*A* and *B*) show tetrads from embryonic mouse (Fig. 10 *A*; and see Franzini-Armstrong et al., 1991) and chick skeletal mus-

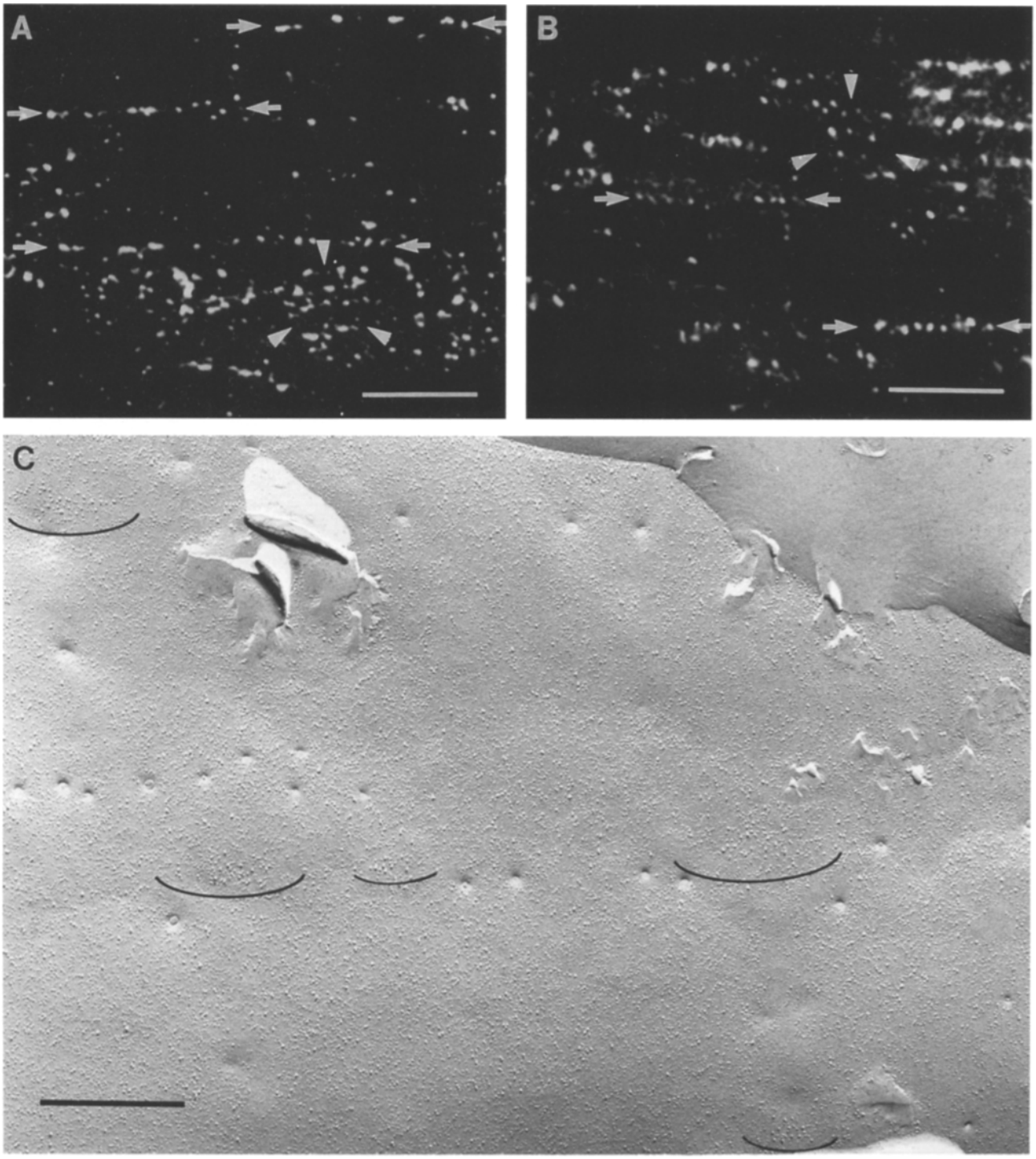

Figure 6. Comparison between immunolabeling for DHPRs (*A*) and RyRs (*B*), and freeze-fracture (*C*), before hatching. Foci of DHPRs and RyRs are located at irregular intervals along the edges of the fibers (between *arrows*) and form irregular patches where the optical section grazes the cell surface (in areas indicated by *three arrowheads*). In freeze-fracture, junctional domains are seen at all levels of the sarcomere. Compare with Fig. 9, showing that peripheral couplings have a widespread distribution before hatching. Bars: (E20, *A* and *B*) 10 μm; (E21, *C*) 0.5 μm.

cle (Fig. 10 *B*; see Takekura et al., 1994*b*). Tetrads (*circles*) are identifiable in both images, despite some distortion during the fracturing process. Contrary to this observation, junctional domains of cardiac muscle (Fig. 10 *C*, *semicircles*) do not show grouping of particles into tetrads.

Particles to Feet Ratios in Skeletal and Cardiac Muscle

In skeletal muscle, junctional tetrads (formed by four membrane particles) are associated with alternate feet, resulting in tetragonal arrays, with a spacing of approximately 41 nm

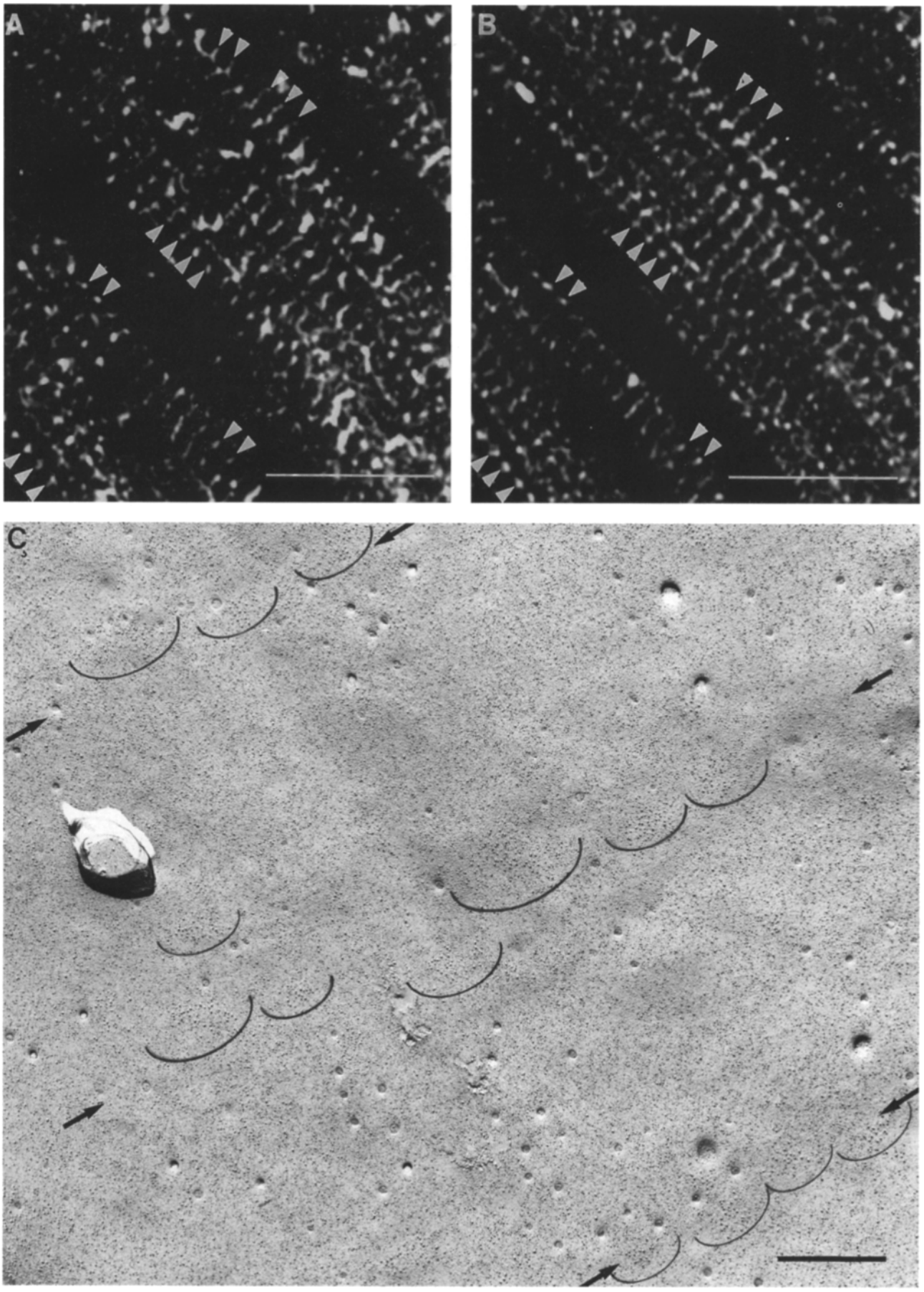

Figure 7. Comparison between double immunolabeling for DHPRs (*A*) and RyR (*B*) and freeze-fracture, shortly after hatching (D6). Foci for the two proteins are located at periodic intervals along the edges of the fibers (*A* and *B*, *arrowheads*) and form transverse bands along the fiber surface. The distance between the bands is the same as the distance between Z lines (visualized by immunolocalization with α-actinin). Most of the foci are colocalized. In freeze-fracture (*C*) the majority of surface domains (*semicircles*) are within narrow transverse strips located in correspondence of the Z lines (between *arrows*). See also Fig. 9. Bars: (*A* and *B*) 25 μm; (*C*) 0.5 μm.

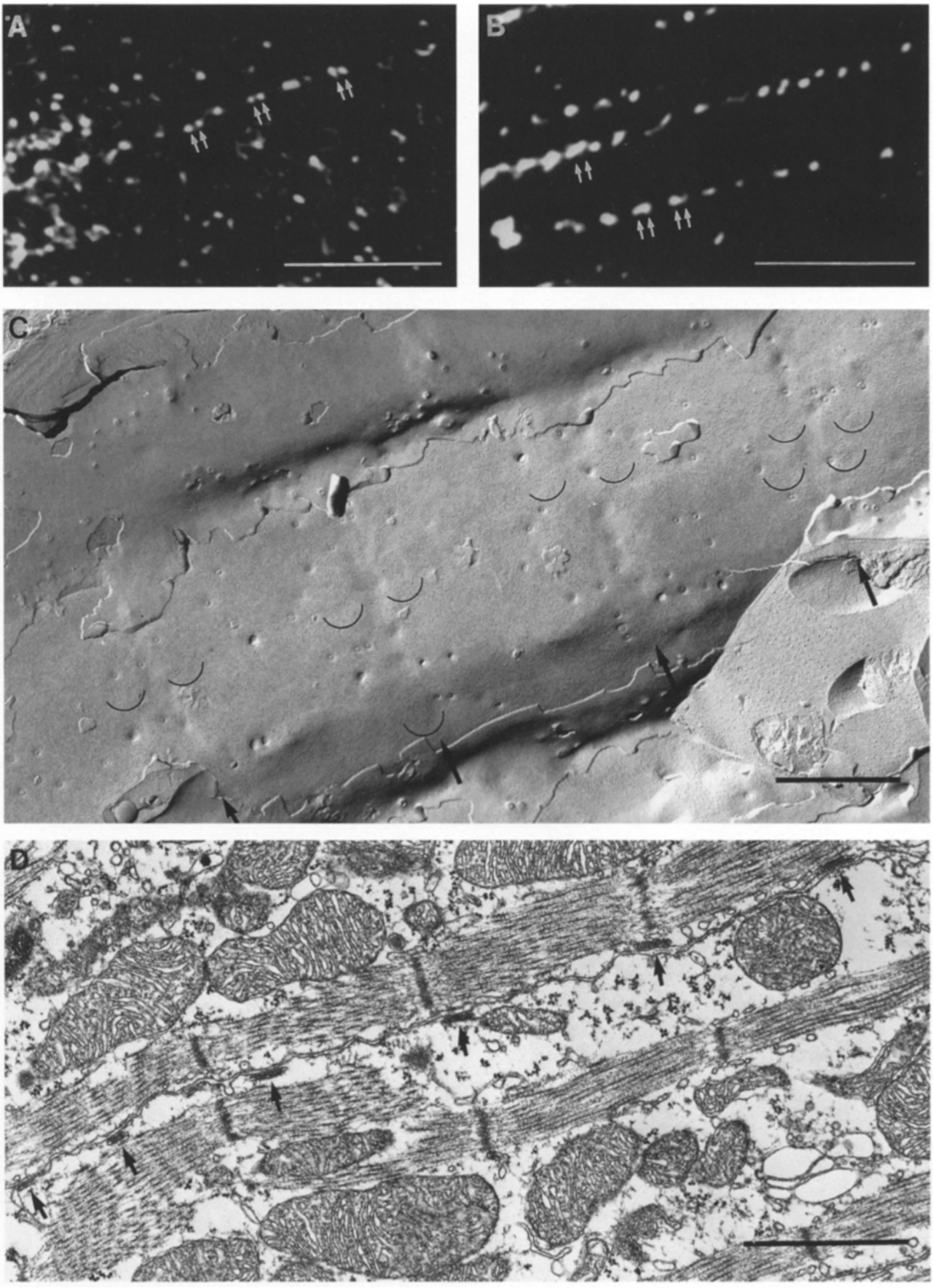

Figure 8. In some, but not all, fibers at D10, DHPR foci (*A*), RyR foci (*B*), and junctional domains (*C*) are located in closely apposed pairs or doublets (*A* and *B*, *double arrows*; *C*, *semicircles*). The junctional domains doublets straddle the Z lines (*C*, *arrows*). In thin section of a fiber at D10 (*D*), five of the seven visible peripheral couplings are in an ideal position (close to the Z line) for forming doublets. Bars: (*A* and *B*) 10 μm; (*C* and *D*) 1 μm.

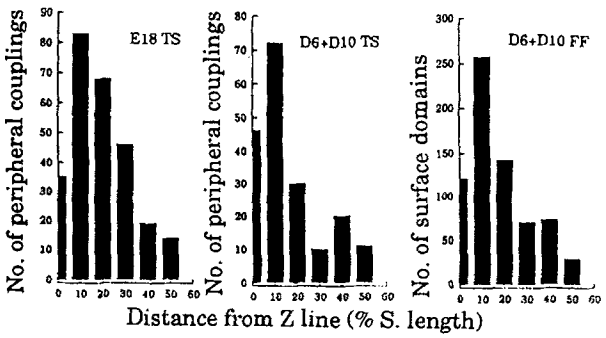

Figure 9. Distribution of peripheral couplings and membrane domains relative to the sarcomere at E18 and D6/D10 (see text). At E18 peripheral couplings, visualized in thin sections (*TS*), have a widespread distribution. At D6 and D10, peripheral couplings (from *TS*) and junctional domains (from freeze-fractures, *FF*) show a preferential location at the Z line and near it.

(Block et al., 1988; Takekura et al., 1994*a*). Feet are also in a tetragonal array, with spacing of 29 nm. From this, the expected density of particles (at four/tetrad) is 2,380/μm^2, and the calculated ratio of particles to feet is 2:1. In reality, however, the density of particles is considerably less, because individual particles and, on occasion, whole tetrads are missing from the arrays. For example, in the best preserved junctional domains of mouse myotubes developing in vivo, 31.5% of the particles are missing on average, giving a density of 1,630 particles/μm^2 (from 300 junctional domains) and an apparent particle/foot ratio of 1.4:1. Although it is clear that some particles are missing from the array due to distortion during fracturing, it is not known whether some of the tetrads were incomplete before fracturing. In cardiac muscle, the measured density of 1,266 particles/μm^2 (see above) gives a particle to foot ratio of 1.06:1 (based on a foot spacing of 29 nm). Due to the lack of arrays, it is not possible to give an estimate of how many particles may be missing as a result of fracturing problems.

Discussion

We have observed co-localization of the α_1 subunit of DHPRs and of RyRs in apposed patches of surface and SR membranes at peripheral couplings of developing chick myocardium. This establishes a similarity between e–c units of cardiac and skeletal muscle, since DHPRs and RyRs are closely apposed in both muscles. An analogous conclusion was inferred in adult guinea pig muscle on the basis of location of the α_2 subunit of DHPR, under the assumption that α_1 and α_2 are colocalized (Lewis-Carl et al., 1995). Although we cannot exclude the possibility that a small number of DHPRs is randomly distributed over the non-junctional plasmalemma, it is clear that most of the inward calcium current through DHPRs must flow into the restricted junctional area where the RyRs are located. A close apposition of DHPRs and RyRs fits the requirements of models of cardiac and invertebrate e–c coupling which are solely dependent on calcium-induced calcium release (Fabiato, 1983; Nabauer et al., 1989; Stern and Lakatta, 1992; Gyorke and Palade, 1993). The models depend on the proximity of I_{Ca} sources, the DHPRs, to the Ca^{2+} release channels, the RyRs, and possibly the existence of a restricted space (Niggli and Lipp, 1993) in order to explain the paradox of the apparently different effects on the RyRs of calcium coming from the out-

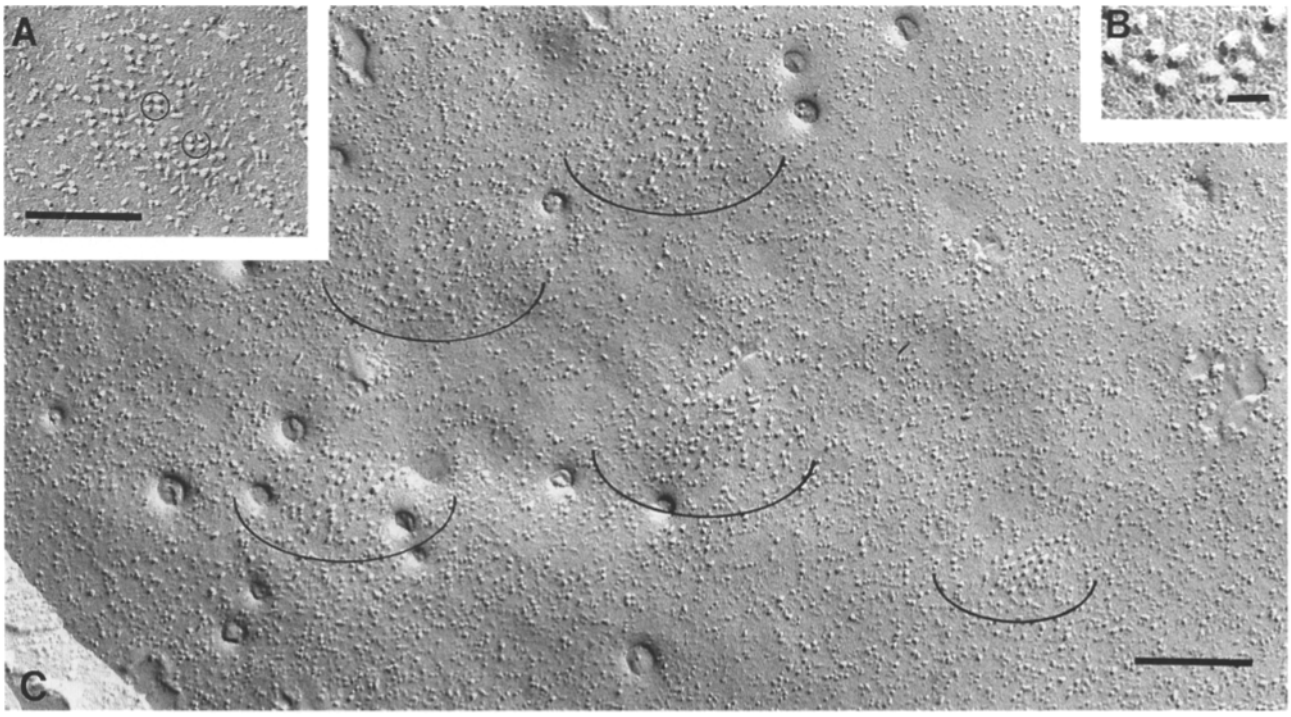

Figure 10. Comparison between junctional domains of skeletal (*A* and *B*) and cardiac (*C*) muscle. In junctional domains from skeletal muscle fibers of embryonic mouse (*A*) and chick (*B*), tetrads, or ordered groupings of four large intramembrane particles (*A*, *circles*), are easily recognizable and form ordered arrays. In cardiac muscle (*C*), the large particles in surface domains (*semicircles*) have a random arrangement and tetrads are not seen. Bars: (*A–C*) 0.2 μm; (*B*) 0.02 μm.

side of the cell, and of calcium released from the SR.

We also demonstrate a close relationship between specialized surface membrane domains containing large intramembraneous particles and the sites of arrays of feet. We propose that the large particles in the junctional domains of cardiac muscle represent DHPRs, based on the similarity of their size to that of the particles composing tetrads in skeletal muscle (Block et al., 1988; Takekura et al., 1994*a*), and on the fact that both particles and DHPRs are located in membrane patches facing the feet/RyRs. While the DHPRs in skeletal muscle apparently are closely linked to the feet, the presumed DHPRs in cardiac muscle are not. Differences in the relationship between DHPRs and RyRs in skeletal and cardiac muscle provide a molecular framework for the known differences in e–c coupling between the two striated muscle types. While in skeletal muscle the voltage sensors (DHPRs) may affect RyR permeability by some direct molecular interaction (Schneider and Chandler, 1973), in cardiac muscle e–c coupling is thought to rely on a less direct means of communication between DHPRs and RyRs (Fabiato, 1983; Niedergerke and Page, 1989).

It is now known that RyRs assemble into arrays independently of other components of the junction and it is thought that some intermediate protein is responsible for holding DHPRs and RyRs in related arrays in skeletal muscle (Caswell et al., 1991). In cardiac muscle, DHPRs and RyRs are located in close proximity. However, there is no apparent relationship between the position of large particles and the feet. It must be assumed that some protein is responsible for anchoring DHPRs at the junction, but perhaps not to the feet. Triadin, the protein thought to mediate DHPRs to RyRs interactions in skeletal muscle triads (Caswell et al., 1991), is also present in cardiac muscle junctions (Brandt et al., 1993) and it may be responsible for DHPRs clustering at peripheral couplings.

The ratio of putative DHPRs (the large intramembrane particles) to feet in cardiac muscle is lower than in skeletal muscle. However, in both muscles, the ratio is higher than that obtained from binding studies with PN200-100 and ryanodine. In cardiac muscle, we obtain a ratio close to 1 (or higher if some particles are missing due to fracturing artifacts), while the binding ratios for various cardiac muscles vary between 0.25–0.27 for rabbit and 0.1 for ferret (Bers and Stiffel, 1993). One major reason for the binding variability, and in part also for the discrepancy between structural and binding data, is the presence of the extended junctional and corbular SR. These vesicles bear feet, but do not associate with T tubules and surface membrane, and thus contribute to the RyR, but not to the DHPR count. However, even taking the corbular SR into consideration, a ratio of 1:4 for DHPRs and feet at SR–T tubule junctions has been proposed for mammalian cardiac muscle (Cannell et al., 1994). This ratio is still considerably lower than predicted from our data, and thus clearly, a precise comparison between structural and biochemical data is not yet possible.

We thank Drs. J. L. Sutko and J. A. Airey for the use of the 34C antibody specific for RyR, and Nosta Glaser for excellent technical help.

Supported by National Institutes of Health ROI HL48093.

Received for publication 13 November 1994 and in revised form 23 January 1995.

References

Airey, J. A., C. F. Beck, K. Murakami, S. J. Tanksley, T. J. Deerinck, M. H. Ellisman, and J. L. Sutko. 1990. Identification and localization of two triad junction foot protein isoforms in mature avian fast twitch skeletal muscle. *J. Biol. Chem.* 265:14187–14194.

Anderson, K., F. A. Lai, Q-Y. Liu, E. Rousseau, H. P. Ericksonand, and G. Meissner. 1989. Structural and functional characterization of the purified cardiac ryanodine receptor-Ca^{2+} release channel complex. *J. Biol. Chem.* 264:1329–1335.

Block, B A., T. Imagawa, K. P. Campbell, and C. Franzini-Armstrong. 1988. Structural evidence for direct interaction between the molecular components of the transverse tubule/sarcoplasmic reticulum junction in skeletal muscle. *J. Cell Biol.* 107:2587–2600.

Bers, D. M., and V. M. Stiffel. 1993. Ratio of ryanodine to dihydropyridine receptors in cardiac and skeletal muscle and implications for e-c coupling. *Am. J. Physiol.* 264:C1587–1593.

Bossen, E. H., J. R. Sommer, and R. A. Waugh. 1978. Comparative stereology of the mouse and finch left ventricle. *Tissue Cell.* 10:773–779.

Brandt, N. R., A. H. Caswell, S. A. Carl, D. G. Ferguson, T. Brandt, J. P. Brunschwig, and A. L. Bassett. 1993. Detection and localization of triadin in rat ventricular muscle. *J. Membr. Biol.* 131:219–228.

Cannell, M. B., H. Cheng, and W. J. Lederer. 1994. Spatial non-uniformities in $[Ca^{2+}]_i$ during excitation-contraction coupling in cardiac myocytes. *Biophys. J.* 67:1942–1956.

Caswell, A. H., N. R. Brandt, J. P. Brunschwig, and S. Purkerson. 1991. Localization and partial characterization of the oligomeric disulfide-linked molecular weight 95,000 protein (triadin) which binds the ryanodine and dihydropyridine receptors in skeletal muscle triadic vesicles. *Biochemistry.* 30:7507–7513.

Coronado, R., J. Morrissette, M. Sukhareve, and D. M. Vaughan. 1994. Structure and function of ryanodine receptors. *Am. J. Physiol.* 266:C1485–C1491.

De Jongh, K. S., D. K. Merrick, and W. A. Catterall. 1989. Subunits of purified calcium channels: a 212-kDa form of α_1 and partial amino acid sequence of a phosphorylation site of an independent β subunit. *Proc. Natl. Acad. Sci. USA.* 86:8585–8589.

Dolber, P. C., and J. R. Sommer. 1984. Corbular sarcoplasmic reticulum of rabbit cardiac muscle. *J. Ultrastr. Res.* 87:190–196.

Fabiato, A. 1983. Calcium-induced release of calcium from cardiac sarcoplasmic reticulum. *Am. J. Physiol.* 245:C1–C14.

Fleischer, S., and M. Inui. 1989. Biochemistry and biophysics of excitation-contraction coupling. *Annu. Rev. Biophys. Biophys. Chem.* 18:333–364.

Flucher, B. E., M. E. Morton, S. C. Froehner, and M. P. Daniels. 1990. Localization of the α_1 and α_2 subunits of the dihydropyridine receptor and ankyrin in skeletal muscle triads. *Neuron.* 5:339–351.

Franzini-Armstrong, C. 1994. The sarcoplasmic reticulum and the transverse tubules. *In* Myology. 2nd edition. A. G. Engel and C. Franzini-Armstrong, editors. Vol. 1:176–199.

Franzini-Armstrong, C., and A. O. Jorgensen. 1994. Structure and development of e-c coupling units in skeletal muscle. *Annu. Rev. Physiol.* 56: 509–534.

Franzini-Armstrong, C., and G. Nunzi. 1983. Junctional feet and particles in the triads of fast-twitch muscle fibers. *J. Muscle Res. Cell Motil.* 4:233–252.

Franzini-Armstrong, C., M. Pincon-Raymond, and F. Rieger. 1991. Muscle fibers from dysgenic mouse *in vivo* lack a surface component of peripheral couplings. *Dev. Biol.* 146:364–376.

Gyorke, S., and P. Palade. 1993. Role of local Ca^{2+} domains in activation of Ca^{2+}-induced Ca^{2+} release in crayfish muscle fibers. *Am. J. Physiol.* 264: C1505–1512.

Inui, M., A. Saito, and S. Fleischer. 1987*a*. Purification of the ryanodine receptor and identity with feet structures of junctional terminal cisternae of sarcoplasmic reticulum from fast skeletal muscle. *J. Biol. Chem.* 262:1740–1747.

Inui, M., A. Saito, and S. Fleischer. 1987*b*. Isolation of the ryanodine receptor from cardiac sarcoplasmic reticulum and identity with the feet structure. *J. Biol. Chem.* 262:15637–15642.

Jewett, P. H., J. R. Sommer, and E. A. Johnson. 1971. Cardiac muscle: its ultrastructure in the finch and hummingbird with special reference to the sarcoplasmic reticulum. *J. Cell Biol.* 59:50–65.

Jorgensen, A. O., R. Broderick, A. P. Somlyo, and A. V. Somlyo. 1988. Two structurally distinct calcium storage sites in rat cardiac sarcoplasmic reticulum: an electron microprobe analysis study. *Circ. Res.* 63:1060–1069.

Jorgensen, A. O., A. C-Y. Shen, W. Arnold, A. T. Leung, and K. P. Campbell. 1989. Subcellular distribution of the 1,4-Dihydropyridine receptor in rabbit skeletal muscle in situ: An immunofluorescence and immunocolloidal gold-labeling study. *J. Cell Biol.* 109:135–147.

Jorgensen, A. O., A. C-Y. Shen, W. Arnold, P. S. McPherson, and K. P. Campbell. 1993. The Ca^{2+} release channel/ryanodine receptor is localized in junctional and corbular sarcoplasmic reticulum in cardiac muscle. *J. Cell Biol.* 120:969–980.

Junker, J., J. R. Sommer, M. Sar, and G. Meissner. 1994. Extended junctional sarcoplasmic reticulum of avian cardiac muscle contains functional ryanodine receptors. *J. Biol. Chem.* 269:1627–1634.

Kawamoto, R. M., J. P. Brunschwig, K. C. Kim, and A. H. Caswell. 1986.

Isolation, localization and characterization of the spanning protein of the skeletal muscle triad. *J. Cell Biol.* 103:1405–1414.

Lai, F. A., H. P. Erickson, E. Rosseau, Q.-Y. Liu, and G. Meissner. 1988. Purification and reconstitution of the calcium release channel from skeletal muscle. *Nature (Lond.).* 331:315–319.

Lewis-Carl, S., K. Felix, A. H. Caswell, N. R. Brandt, W. J. Ball, P. L. Vaghy, G. Meissner, and D. G. Ferguson. 1995. Immunolocalization of sarcolemmal dihydropyridine receptor and sarcoplasmic reticular triadin and ryanodine receptor in rabbit ventricle and atrium. *J. Cell Biol.* 129:673–682.

Meissner, G. 1994. Ryanodine receptor/Ca^{2+} release channels and their regulation by endogenous effectors. *Annu. Rev. Physiol.* 56:485–508.

Nabauer, M., G. Gallewaert, L. Cleemann, and M. Morad. 1989. Regulation of calcium release is gated by calcium current, not gating charge, in cardiac myocytes. *Science (Wash. DC).* 244:800–803.

Niedergerke, R., and S. Page. 1989. Receptor controlled calcium discharge in frog heart cells. *Quart. J. Exp. Physiol.* 74:987–1002.

Niggli, E., and P. Lipp. 1993. Subcellular restricted spaces: significance for cell signaling and excitation-contraction coupling. *J. Muscle Res. Cell Motil.* 14:288–291.

Ogawa, Y. 1994. Role of ryanodine receptors. *Crit. Revs. Biochem. Mol. Biol.* 29:229–274.

Pozzan, T., R. Rizzuto, P. Volpe, and J. Meldolesi. 1994. *Physiol. Rev.* 74:595–636.

Rios, E., and G. Brum. 1987. Involvement of dihydropyridine receptors in excitation-contraction coupling in skeletal muscle. *Nature (Lond.).* 325: 717–720.

Rios, E., J. Ma, and A. Gonzales. 1991. The mechanical hypothesis of excitation contraction coupling. *J. Muscle Res. Cell Motil.* 12:127–135.

Schneider, M. F., and W. K. Chandler. 1973. Voltage dependence charge movement in skeletal muscle: a possible step in excitation contraction coupling. *Nature (Lond.).* 242:244–246.

Sommer, J. R., and E. A. Johnson. 1979. Ultrastructure of cardiac muscle. *In* Handbook of Physiology. Section 2: The Cardiovascular system. Vol. 1. The Heart. R. M. Berne, N. Sperelakis, and S. R. Geiger, editors. American Physiological Society, Bethesda, MD. 113–187.

Sommer, J. R., E. Bossen, H. Dalen, P. Dolber, T. High, P. Jewett, E. A. Johnson, J. Junker, S. Leonard, R. Nassar, B. Scherer, M. Spach, T. Spray, I. Taylor, N. R. Wallace, and R. Waugh. 1991. To excite a heart: a bird's view. *Acta Physiol. Scand.* 142 (suppl. 599):5–21.

Sorrentino, V., and P. Volpe. 1993. Ryanodine receptors: how many, where and why? *Trends Pharmacol. Sci.* 14:98–105.

Stern, M. D., and E. G. Lakatta. 1992. Excitation-contraction coupling in the heart: the state of the question. *FASEB (Fed. Am. Soc. Exp. Biol.) J.* 6:3092–3100.

Takahashi, M., and W. A. Catterall. 1987. Dihydropyridine-sensitive calcium channels in cardiac and skeletal muscle membranes: studies with antibodies against α subunits. *Biochemistry.* 26:5518–5526.

Takekura, H., L. Bennet, T. Tanabe, K. G. Beam, and C. Franzini-Armstrong. 1994*a*. Restoration of junctional tetrads in dysgenic myotubes by dihydropyridine receptor cDNA. *Biophys. J.* 67:793–804.

Takekura, H., X.-H. Sun, and C. Franzini-Armstrong. 1994*b*. Development of the excitation-contraction coupling apparatus in skeletal muscle. Peripheral and internal calcium release units are formed sequentially. *J. Muscle Res. Cell Motility.* 15:102–118.

Tanabe, T., K. G. Beam, J. A. Powell, and S. Numa. 1988. Restoration of excitation-contraction coupling and slow calcium current in dysgenic muscle by dihydropyridine receptor complementary DNA. *Nature (Lond.).* 336: 134–139.

Yoshida, A., M. Takahashi, S. Nishimura, H. Takeshima, and S. Kokubun. 1992. Cyclic phosphorylation and regulation of the cardiac dihydropyridine-sensitive Ca^{2+} channel. *FEBS (Fed. Eur. Biochem. Soc.) Lett.* 309:343–349.

Yuan, S., W. Arnold, and A. O. Jorgensen. 1991. Biogenesis of transverse tubules and triads: immunolocalization of the 1,4-dihydropyridine receptor, TS28, and the ryanodine receptor in rabbit skeletal muscle developing in situ. *J. Cell Biol.* 112:289–301.